

Serveur Académique Lausannois SERVAL serval.unil.ch

Author Manuscript

Faculty of Biology and Medicine Publication

This paper has been peer-reviewed but does not include the final publisher proof-corrections or journal pagination.

Published in final edited form as:

Title: Prediction of multiple infections after severe burn trauma: a prospective cohort study.

Authors: Yan S, Tsurumi A, Que YA, Ryan CM, Bandyopadhaya A, Morgan AA, Flaherty PJ, Tompkins RG, Rahme LG

Journal: Annals of surgery

Year: 2015 Apr

Volume: 261

Issue: 4

Pages: 781-92

DOI: 10.1097/SLA.0000000000000759

In the absence of a copyright statement, users should assume that standard copyright protection applies, unless the article contains an explicit statement to the contrary. In case of doubt, contact the journal publisher to verify the copyright status of an article.



Published in final edited form as:

Ann Surg. 2015 April ; 261(4): 781–792. doi:10.1097/SLA.0000000000000759.

Prediction of Multiple Infections After Severe Burn Trauma: a Prospective Cohort Study

Shuangchun Yan, PhD^{1,2,3}, Amy Tsurumi, PhD^{1,2,3}, Yok-Ai Que, MD, PhD⁴, Colleen M. Ryan, MD^{1,3}, Arunava Bandyopadhyaya, PhD^{1,2,3}, Alexander A. Morgan, PhD⁷, Patrick J. Flaherty, PhD^{5,6}, Ronald G. Tompkins, MD, ScD¹, and Laurence G. Rahme, MS, PhD^{1,2,3}

¹Department of Surgery, Massachusetts General Hospital, Harvard Medical School, Boston, Massachusetts, United States of America ²Department of Microbiology and Immunobiology, Harvard Medical School, Boston, Massachusetts, United States of America ³Shriners Hospitals for Children Boston, Boston, Massachusetts, United States of America ⁴Department of Fundamental Microbiology, University of Lausanne, Lausanne, 1015, Switzerland ⁵Department of Biomedical Engineering, Worcester Polytechnic Institute, Worcester, Massachusetts, United States of America ⁶Program in Bioinformatics and Computational Biology, Worcester Polytechnic Institute, Worcester, Massachusetts, United States of America ⁷Department of Biochemistry & Stanford Genome Technology Center, Stanford University School of Medicine, Palo Alto, California, United States of America

Abstract

Objective—To develop predictive models for early triage of burn patients based on hyper-susceptibility to repeated infections.

Background—Infection remains a major cause of mortality and morbidity after severe trauma, demanding new strategies to combat infections. Models for infection prediction are lacking.

Methods—Secondary analysis of 459 burn patients (16 years old) with 20% total body surface area burns recruited from six US burn centers. We compared blood transcriptomes with a 180-h cut-off on the injury-to-transcriptome interval of 47 patients (1 infection episode) to those of 66 hyper-susceptible patients (multiple [2] infection episodes [MIE]). We used LASSO regression to select biomarkers and multivariate logistic regression to built models, accuracy of which were assessed by area under receiver operating characteristic curve (AUROC) and cross-validation.

Results—Three predictive models were developed covariates of: (1) clinical characteristics; (2) expression profiles of 14 genomic probes; (3) combining (1) and (2). The genomic and clinical models were highly predictive of MIE status (AUROC_{Genomic} = 0.946 [95% CI, 0.906–0.986]; AUROC_{Clinical} = 0.864 [CI, 0.794–0.933]; AUROC_{Genomic}/AUROC_{Clinical} *P* = 0.044). Combined

Corresponding author: Laurence G. Rahme, PhD, MS, Harvard Medical School, Massachusetts General Hospital, rahme@molbio.mgh.harvard.edu, Tel. +1 (617) 724-5003; Fax +1 (617) 724-8558.

Publisher's Disclaimer: Disclaimer

The Inflammation and the Host Response to Injury “Glue Grant” program is supported by the National Institute of General Medical Sciences. This manuscript was prepared using a dataset obtained from the Glue Grant program and does not necessarily reflect the opinions or views of the Inflammation and the Host Response to Injury Investigators or the NIGMS.

model has an increased AUROC_{Combined} of 0.967 (CI, 0.940–0.993) compared to the individual models (AUROC_{Combined}/AUROC_{Clinical} $P = 0.0069$). Hyper-susceptible patients show early alterations in immune-related signaling pathways, epigenetic modulation and chromatin remodeling.

Conclusions—Early triage of burn patients more susceptible to infections can be made using clinical characteristics and/or genomic signatures. Genomic signature suggests new insights into the pathophysiology of hyper-susceptibility to infection may lead to novel potential therapeutic or prophylactic targets.

INTRODUCTION

Although several studies have found association between specific risk factors or clinical characteristics with mortality after trauma,^{1–4} studies attempting to apply those clinical characteristics or genomic biomarkers to appreciate susceptibility to infection and build predictive models are currently lacking. Improvements in early care and trauma centers have reduced early mortality considerably.^{3,5} However, severe trauma, such as burn trauma, cause immunosuppression which predispose patients to infections. Despite all medical improvements, infections remain a major cause of critical injury-related morbidity and mortality, and recurrent sepsis predisposes patients to multiple organ failure, lengthens hospital stays, and increases costs.⁶ Therefore, improvements in prevention and treatment of infections are increasingly important.^{7,8} Moreover, the rapid emergence of multi-(MDR) or pan-drug resistant (PDR) pathogens that cause highly problematic acute, persistent or relapsing infections pose a dire threat to healthcare, especially among trauma and surgical patients.^{9,10} The increased use of antibiotics has further accelerated their emergence,^{11–13} and also increased the challenge of treating polymicrobial wound infections.^{14,15} Due to the paucity of novel anti-infectives in development, further improvement in patient care and treatment efficacy may rely heavily on optimizing existing strategies and promoting patients-tailored therapies.^{16–18}

Successful personalized approach requires rigorous triaging: early and accurate identification of patients more susceptible to infections could help tailor the anti-infective treatments,^{19,20} and especially to elaborate long-term treatment plan. Future successful clinical trials aiming to improve sepsis outcome may also rely on biomarkers to identify the right patients for the right treatment.^{21,22} Several studies have reported risk factors associated with increased probability of infection and sepsis in trauma patients,^{23–26} but no specific predictive model has been developed. Existing plasma biomarkers such as C-reactive protein (CRP) and procalcitonin (PCT) are mainly used to diagnose sepsis^{27,28} rather than reflective of susceptibility or health status. The clinical characteristics measurable rapidly upon admission are the current gold standard for prognosis of general patient's outcome.

As trauma promotes susceptibility to infection and genomic signatures appear to play an increasingly promising role in prognosis,^{26,29} we analyzed the blood transcriptome and clinical characteristics data of 113 patients from the 573 thermally injured patients enrolled in the Inflammation and the Host Response to Injury study. Using clinical characteristics

available upon admission and early genomic signatures, we developed novel predictive models that would permit early identification of burn patients at high risk of developing repeated infection indicative of an early hyper-susceptible state. The genomic signature suggests new mechanistic aspects for susceptibility to infection after burn trauma.

METHODS

Subject Recruitment and Sample Selection

This study was conducted via secondary use of the clinical and genomic data of the Inflammation and the Host Response to Injury Study (“Glue Grant”). Briefly, 573 burn patients with minimum 20% total burn surface area (TBSA) were enrolled from six institutions between 2003 and 2009 in a prospective, longitudinal study. RNA of leucocytes isolated from whole blood samples were extracted for transcriptome analysis using Affymetrix GeneChip Human Genome U133 Plus 2.0 microarrays at University of Florida–Gainesville, as described previously.³⁰ The complete inclusion/exclusion criteria are described elsewhere.³¹ Permission for this secondary use of the de-identified data was obtained from the Massachusetts General Hospital Institutional Review Board (MGH IRB protocol 2008-P-000629/1).

Our patient inclusion process is summarized in Figure 1. From 573 potential patients in the data pool, we selected for patients that were at least 16 years old with early transcriptome data. We set a 180-h cut-off limit on the injury-to-transcriptome interval to include only samples that were obtained early relative to the recovery process, while still allowing enough samples to remain eligible for biomarker discovery. If multiple blood samples were collected from a patient, only the earliest eligible sample was included. We excluded patients who died within 9 days of blood collection and had fewer than two infection episodes during this time window (Figure 1; Figure 1A). Our method for collection of data related to clinical characteristics is described elsewhere.³¹ To enable direct comparisons, as well as combination of clinical and genomic prediction, we used the same set of patients for both our clinical characteristic and our genomic signature prediction models.

Definition of Outcomes

We defined infections according to the information collected in the Glue Grant database based on previously described standards.³² Infection episodes were quantified for each patient for up to 60 days after blood sample collection. We developed a decision tree (Figure 1B; Supplemental Digital Content[SDC] Table 1) for evaluating each record based on: (1) time of infection; (2) type of infection; and (3) the pathogen(s) isolated. Since no genotyping data of the isolated pathogen species were available, we were unable to classify whether a later episode was caused by the same strain isolated earlier. However, once a record was counted, the infection type and isolated pathogen combination (e.g. *Pseudomonas aeruginosa* + lung) was put on a “waiting list” for the next 6 days, which likely reduced the likelihood of an infection episode caused by the same isolate from being counted. Subsequent records that were part of the same infection episode were thereby omitted. The patients were separated into two groups based on susceptibility to infection, measured by the number of independent infection episodes recorded. We defined patients with 1 infection

episodes as the less susceptible control group (N = 47), and patients with ≥ 2 (multiple) infection episodes (MIE) as the hyper-susceptible case group (N = 66).

Microarray Processing and Filtering

Raw microarray data (.CEL files) were downloaded from the Glue Grant website (<http://www.gluegrant.org/trdb/>) and filtered using the steps outlined in Figure 1, SDC Table 1 and Figure 1B. We used the *gcrma*³³ package on the R/Bioconductor platform³⁴ to normalize 124 blood samples from 124 eligible patients collected within 180 h post-injury. Samples identified as outliers by *arrayQualityMetrics*³⁵ were excluded from subsequent analysis. One patient was removed due to incompleteness of clinical data. Two patients' datasets were discarded due to mortality within 9 days after sample collection. After these filtration steps, 113 blood samples were deemed suitable high-quality microarray data sets for subsequent functional analyses, biomarker discovery, and modeling.

We used the *EMA* package³⁶ in R software to filter outlying or information-poor probe sets. We eliminated probe sets with a maximum \log_2 expression value below 3.5, reducing the number of probe sets from 54,675 to 26,107. Using *limma* package,³⁷ we selected 1142 probe sets with an at least 1.5-fold difference between less susceptible patients and hyper-susceptible patients and with an average expression level of at least 3 for functional analyses and biomarker panel selection process.

Statistical Analysis

Clinical data set—Continuous variables are reported as means (standard deviations), or as medians with inter-quartile ranges (IQRs) as indicated. Categorical variables are reported as frequencies and percentages. Demographic variables between less susceptible and hyper-susceptible patients were tested for statistical difference with a Wilcoxon rank sums test, a Chi-square test, or a Fisher's exact test as appropriate. Statistical significance was accepted at $P < 0.05$ (two-tailed when appropriate).

Body mass index (BMI) was calculated as $\text{weight}/\text{height}^2$ (kg/m^2). For patients ≥ 20 years old, BMI categories of underweight, healthy, overweight and obese were defined according to BMI numbers: <18.5, 18.5–24.9, 25–29.9, and ≥ 30, respectively; whereas for patients <20 years old, the same BMI categories were defined using percentile ranking based on Centers for Disease Control and Prevention BMI-for-age growth charts: <5th percentile, 5th to <85th percentile, 85th to <95th percentile, and ≥ 95th percentile, respectively.

Genomic data set—In our evaluation of significant expression differences between less susceptible and hyper-susceptible patients, Benjamini-Hochberg multiple-comparison adjustments were applied to control for false discovery rate.

Development of the clinical predictive models—We implemented stepwise logistic regression with an entry level of 0.3 and a stay level of 0.25 to identify significant predictor variables among clinical covariates relevant to the outcome variable of MIE: TBSA, age, BMI, and the presence of inhalation injury. We determined predictive power by calculating

area under receiver operating characteristic curve (AUROC), reported with 95% confidence intervals (CIs).

Development of the genomic predictive models—We used the LASSO regularized regression method³⁸ implemented in the glmnet package³⁹ in R software to identify probe sets that collectively predicted the likelihood of MIE. We used 10-fold cross-validation (CV) to select the optimal value of LASSO penalty weighting, λ . The value of λ that gave the minimum average binomial deviance plus 1 standard error on the test set, λ_{1se} , was used to select probe sets (Figure 3A). λ_{1se} is a stronger penalty parameter to guard against over-fitting than λ_{min} , which minimizes the average binomial deviance of CV (Figure 3B). This 10-fold CV process was repeated 100 times to generate 100 λ_{1se} values. The median λ_{1se} , 0.0940, yielded selection of a 14-probe-set biomarker panel (Figure 3C; Table 2). Logistic regression was performed to model the MIE outcome with the \log_2 expression values of the 14 probe sets as explanatory variables. Furthermore, we conducted multivariate logistic regression with the clinical covariates TBSA, age, and inhalation injury together with the 14 probe sets for the outcome variable of MIE. Leave-one-out cross-validation was used to assess the degree of over-fitting and model performance.

Functional Analysis

Functional and pathway analyses were conducted using Ingenuity IPA (Ingenuity® Systems, www.ingenuity.com) and DAVID.⁴⁰

Software Platform and Package Versions

R (version 2.15.*); EMA package for R (version 1.3.2); pROC package for R (version 1.5.4); limma package for R (version 3.14.4); glmnet package for R (version 1.9-3); arrayQualityMetrics package for R (version 3.14.0); gcrma package for R (version 2.30.0); JMP Pro 10 and SAS 9.3 (SAS Institute Inc., North Carolina, USA).

RESULTS

Clinical Characteristics

From a pool of 573 patients, 124 met our inclusion criteria, of which 11 were unsuitable for modeling, leaving a cohort of 113 patients (Figure 1), including 47 patients less susceptible to infection (control group with 1 infection episodes) and 66 hyper-susceptible patients (case group with multiple [2] infection episodes [MIE]). The demographics, injury characteristics, and outcomes of these 113 patients are summarized in Table 1.

From 612 microbiological records for the 113 patients in the final cohort, we identified 325 independent infection episodes, 107 (32.9%) of which are polymicrobial at the species level. Twenty-four patients had no infection episodes, 23 had one episode, and 66 had MIE. The less susceptible and hyper-susceptible patients show significantly different clinical characteristics (Table 1). Relative to the control group, hyper-susceptible patients were slightly older (mean, 38.2, SD 16.4 vs 37.0, SD 14.6), had higher TBSA (46%, IQR 35–71 vs 32%, IQR 23–41, $P < 0.0001$), had more inhalation injuries (41/66 [62.1%] vs 8/47 [17.0%], $P < 0.0001$) and were more severely ill (according to their APACHE II score 24,

IQR 18–29 vs 13, IQR 9–20, $P < 0.0001$). They also had longer hospital stays (median, 60, IQR 33–71 vs 20, IQR 15–30, $P < 0.0001$), more days on mechanical ventilation (median, 28, IQR 13–40 vs 2, IQR 0–5, $P < 0.0001$), and had a higher mortality (18/66 [27.3%] vs 3/47 [6.4%], $P = 0.0029$) (Table 1). The median post-injury interval for the second episode in the case group was 15 days (IQR, 10–20; range, 3–43), a time window that provides opportunity for prophylactic intervention.

Inhalation injury significantly increased the risk of developing MIE and may be related to pneumonia risk in particular: 78.8% of hyper-susceptible patients had pneumonia vs 10.6% of controls; among cases, 84.7% had both MIE and inhalation injuries, 67.4% had both pneumonia and inhalation injuries. Interestingly, 4/5 of underweight patients had MIE (Table 1), supporting the notion that being overweight and mild obesity may be protective against post-injury infection whereas being underweight increases risk.^{32,41}

Burn wound infection and nosocomial pneumonia were the most frequent types of infection observed (Table 1; Figure 2A). *Pseudomonas aeruginosa* and Staphylococci (both *Staphylococcus aureus* and coagulase negative Staphylococci) were the most commonly isolated micro-organisms (Table 1; Figure 2B). *P. aeruginosa* and *Acinetobacter* infections were more common among patients with MIE than controls, suggesting that hyper-susceptible patients were even more susceptible to nosocomial Gram-negative pathogens.

MIE Prediction from Clinical Characteristics

We used stepwise logistic regression to select covariates for modeling from TBSA, age, BMI, and the presence of inhalation injury. The final multivariate logistic regression model included three covariates: TBSA, age, and inhalation injury, which were significant independent predictors of MIE. The AUROC, CV AUROC, sensitivity, and specificity values for the clinical characteristics model are 0.845 (95% CI, 0.773–0.916), 0.838 (95% CI, 0.762–0.914), 0.803 (95% CI, 0.683–0.887), and 0.745 (95% CI, 0.594–0.856), respectively (Figure 3). The model's positive and negative predictive values were 0.815 (95% CI, 0.696–0.843) and 0.729 (95% CI, 0.579–0.843), respectively. Inhalation injury significantly increased MIE incidence (odds ratio [OR], 6.942; 95% CI, 2.482–19.417). Patients who had inhalation injuries were twice as likely to get pneumonia compared to those without them (risk ratio [RR], 2.05; 95% CI, 1.37–3.07). Among those who had inhalation injuries, 67.4% had pneumonia, and 83.67% had MIE. TBSA (OR, 1.078; 95% CI, 1.040–1.118) and age (OR, 1.040; 95% CI, 1.006–1.075) were also associated with increased infection susceptibility.

MIE Prediction from Genomic Biomarkers in Blood

Ten-fold CV using LASSO regularized regression³⁸ of the 1142 probe sets that presented a minimum of 1.5-fold change between the two patient groups yielded a minimal set of 14 predictors (probe sets) that together optimized the fit of the model (Figure 4A and 4B). Of these 14 probe sets—which mapped to 12 genes—4 were upregulated and 10 were down-regulated (Table 2, all $P < 0.01$; see Figure 4C for heat map and clustering of patients and biomarkers; see Figure 2 for expression profiles of each probe set). The biological processes associated with each probe set are presented in Table 3 together with the coefficients of the

biomarker panel logistic regression model (model intercept = 0.7449; SDC Table 6). The AUROC, CV AUROC, sensitivity, and specificity values for the resulting genomic signature model are 0.946 (95% CI, 0.906–0.986), 0.872 (95% CI, 0.804 – 0.940), 0.924 (95% CI, 0.825–0.972), and 0.830 (95% CI, 0.687–0.919), respectively (Figure 3), confirming the model to be highly sensitive and specific. The positive and negative predictive values of the model were 0.884 (95% CI, 0.779–0.945) and 0.886 (95% CI, 0.746–0.957), respectively. We compared each patient’s probability of developing MIE estimated from our clinical or genomic biomarker logistic regression models with each of the observed outcomes, using cut-off points of 30% to 70% as being uncertain. We found that the clinical model correctly predicted outcomes of 73 (65%) patients with certainty. Comparatively, the genomic biomarker model correctly predicted 90 (80%) patients with certainty, showing a 15% improvement over the clinical model. Both models misclassified 9 patients (8%). Collectively, these data suggest that genomic biomarkers may complement triage by clinical characteristics and enhance early prediction of a patient’s likelihood to develop MIE.

MIE Prediction from a Combined Model

A multivariate logistic model that included the aforementioned clinical covariates (TBISA, age, presence of inhalation injury) and genomic biomarkers resulted in an AUROC (0.967; 95% CI, 0.940–0.993) that was significantly greater than that for the clinical model ($P = 0.0069$), but not significantly different from that of the genomic biomarker panel model (Figure 3). The positive and negative predictive values of the combined model were 0.881 (95% CI, 0.773–0.943) and 0.848 (95% CI, 0.705–0.932), respectively. The estimates of the above models are listed in SDC Table 6.

Functional and Canonical Pathway Changes in Patients with MIE Revealed by Transcriptome Data Analysis

The 1142 probe sets showing a minimum of 1.5-fold change in hyper-susceptible patients versus less susceptible patients were mapped to 844 annotated genes. We identified functionally related genes among these 884 genes using Gene Ontology (GO). Subsequent analysis of the changes in canonical pathways and functions linked to these 844 genes indicated that hyper-susceptible patients’ transcriptomes demonstrated the following early functional changes relative to control transcriptomes: (1) early activation of immune cells, increased chemotaxis and trafficking; (2) decreased expansion of leukocytes, thymocytes, and number of phagocytes, and increased cell death and apoptosis; and (3) suppression of immune cell activation and lymphoid organ development (Table 2). The 1142 probe sets showed enrichment in four main gene ontology biological process categories: (1) immune response; (2) epigenetic modulation of gene expression; (3) transcription; and (4) metabolism (SDC Tables 2). Functional enrichment clustering is also in agreement with the enrichment of the 4 functional groups (SDC Table 3). The top 30 affected pathways were mainly involved in immune cell signaling and cytokine signaling (Figure 5). Canonical pathway analysis using IPA software (Figure 5) largely agrees with KEGG pathway enrichment analysis using DAVID (SDC Table 5), providing additional confidence. Overall, many of the predicted functional changes (Table 2) are downstream of the affected canonical pathways (Figure 5; SDC Table 5).

Canonical Pathways and T-cell Signaling—Significant changes in IL-8 signaling (17 upregulated and 12 down-regulated genes [17 up/12 down]), Gαq signaling (16 up/9 down), Rho family GTPase signaling (20 up/10 down) and integrin signaling (21 up/9 down) suggest that the adhesion and migration of leukocytes are affected (Table 2; SDC Table 3; and Figure 5). The changes in chemotaxis may be partially caused by the presence of bacteria at wound site, as fMLP signaling pathway (12 up/8 down) suggests. Genes involved in phospholipase C signaling, a regulator of chemotactic response are differentially expressed (20 up/16 down). The increased cell movement, adhesion, and chemotaxis are related to phagocytosis process (e.g. FcγR-mediated phagocytosis, SDC Table 6), clearance of the pathogen from the site of infection, and induced by host damage associated molecular patterns (DAMP).

We found strong evidence that T-cells were also differentially regulated in case patients. Several pathways, including T-cell receptors (TCR) (7 up/16 down), JAK-STAT signaling (9 up/7 down), PKCθ signaling (8 up/15 down), and IL-6 signaling pathway (13 up/6 down) are known to regulate T-cell differentiation, activation, and cytokine production. Changes in iCOS-iCOSL signaling (10 up/14 down), CD28 signaling (11 up/16 down), and IL-2 signaling (7 up/7 down), indicate that T helper cell maturation and proliferation were likely affected. In summary, patient transcriptome data is consistent with compromised cellular immune responses mediated by impaired T-cells signaling.

Functional Enrichment in Histone Modification and Chromatin Remodeling—

We found evidence for dramatic epigenetic changes in leukocytes that long precede patient outcome of MIE. Functions related to epigenetic modulation were commonly enriched in our functional enrichment analyses (SDC Tables 2, 3, and 4). Notably, 42 probe sets (39 genes) have functional annotation associated with chromatin remodeling and histone modifications (SDC Table 4). Two genes from the biomarker panel involved in epigenetic modulation were found to be down-regulated in the case group with MIE: *WHSC1L1*, which encodes a histone lysine methyltransferase; and *SMARCA4*, which encodes an ATP-dependent helicase related to the SWI/SNF chromatin remodeling factor. A multitude of differentially expressed genes encoding histone post-translational modifiers as well as key components of the nucleosome remodeling complex mediating ATP-dependent nucleosome sliding, including *SMARCC1*, *SMARCA4*, *CHD2* and *CHD9*, were down-regulated (SDC Table 4). Other notable histone methyltransferases/demethylases differentially expressed include *KDM4*, *KDM5C*, *KDM6*, *PRDM5*, *SETD2*, *SETDB2*, and *SUZ12*. Genes coding for histone deacetylases/acetyltransferases and associated factors including *HDAC9*, *KAT6A* and *EP400* were down-regulated and histone acetylation recognizing bromodomain containing protein, *BRD2*, was upregulated in the case group. Furthermore, critical non-histone heterochromatin proteins HP1-α and -γ were down-regulated, as well as core histone cluster. Taken together, our data may suggest a global loss of heterochromatin and genome instability, as well as probable gene-specific transcriptional deregulation in hyper-susceptible patients compared to controls.

DISCUSSION

The work presented reports novel predictive models for hyper-susceptibility to infection among traumatically injured patients, using genomic biomarkers and/or clinical characteristics that have not been used to build statistical prognostic models for the purpose of predicting infection outcomes. We provide evidence that our models can identify burn patients at high risk of developing repeated infections indicative of their hyper-susceptible state. To our knowledge, this work is the first to describe such models in trauma patients, and the first to describe functional transcriptome data of burn patients in relation to infections. The prediction accuracy of hyper-susceptibility to MIE is significantly increased over clinical markers when the genomic signature is used, providing strong evidence of the promising role of genomic biomarkers in prognosis even when used alone. By combining the biomarker panel with clinical characteristics, we demonstrated even better prediction accuracy, supporting the tremendous potential of using genomic signature to increase confidence in data used for treatment decision-making.

Clinical Implications

We identified two distinct patient groups with different genomic signatures and clinical characteristics, essentially allowing the rapid identification of patients with a high risk of developing MIE following burn trauma. Although burn patients generally suffer from immunosuppression, clinical experience and our data suggest that the severity of immunosuppression and infection outcome vary. These data suggest that patients could potentially receive personalized therapy depending on their susceptibility to infection, triaged by physical exam and a blood test on admission. This information could facilitate the determination of appropriate treatment courses, particularly in regards to antibiotic use, allowing for selective use of prophylactic antibiotics and more objective justification of length of treatment courses. For the patient, this could limit complications related to unneeded antibiotics, reduce the burden of lines needed to deliver the antibiotics, and streamline hospital care. For the population, this could promote antibiotic stewardship, help stem the emergence of resistant organisms, and reduce the cost of care.

Mechanistic Aspects

Genomic signatures provide insight into the molecular mechanisms of the more susceptible health status, and may aid in the discovery of novel therapeutic targets. Our findings point to novel potential targets for the prevention and/or early treatment of infections. Functional analyses of the 1142 biomarker candidates suggest new aspects into the pathophysiology of susceptibility to MIE after trauma. Susceptibility to MIE was associated with early alterations in numerous signaling pathways related to innate and adaptive immune responses, and changes in epigenetic modulation and metabolism.

Some of our findings are consistent with previous literature. For instance, upregulation of *THBS1* (thrombospondin 1), to which 3/14 of the biomarker probe sets were mapped, has been associated with complicated recovery in blunt trauma patients,²⁹ supporting the broad applicability of our approach and findings. The discovery of *THBS1* also supports the potential biological relevance of our biomarkers. Indeed, increased expression of mouse

homologue *Thbs1* has been reported to be associated with infection,⁴² thrombosis, and increased lipopolysaccharide-induced mortality. Interestingly, *Thbs1* $-/-$ knockout mice show reduced susceptibility to peritoneal sepsis,⁴³ whereas *Thbs1* over-expressing transgenic mice show impaired wound healing associated with wound angiogenesis inhibition.⁴⁴ THBS1 in human wounds could be functioning to provide adhesion target for pathogens through promotion of thrombosis,⁴⁵ and/or delayed wound healing, which could lead to increased susceptibility to infection. Thus, building on convergent findings in humans and mice, our data confirm that processes related to coagulation play important roles in sepsis, and suggest that THBS1 could be a novel target for sepsis prevention and treatment.

We showed evidence for increased chemotaxis, cell adhesion, and migration of immune cells, and simultaneously, decreased expansion of immune cells and development of lymphatic system components. This seeming contradiction may well be the consequences of dysfunctional immune system and cytokine signaling, especially in T-cells.

Our data suggest that epigenetic changes occur early on, rather than mainly as a consequence of septic shock. Epigenetic regulation of immune system is a common mechanism for gene expression regulation and it plays a role in long-term immunosuppression after sepsis.⁴⁶ Tightly regulated chromatin remodeling is required for transcriptional regulation, which is vital for proper host immune and inflammatory responses.⁴⁷ Among the genes associated with epigenetic regulations, several have confirmed roles in immune responses, such as *KAT6A* and *KDM6B* (SDC Table 4).^{46,48-50} Furthermore, our data further supports the notion that genes related to cell-cycle control and DNA repair have roles in both immune responses and tumorigenesis. In summary, the dramatic epigenetic changes could potentially explain why our biomarker panel could predict MIE that occurred weeks later, and the underlying mechanisms that favor infections by Gram-negative opportunistic pathogens.

Implications for Future Research

With the aforementioned clinical implications and mechanistic aspects, our findings lay the groundwork for a new pathway of investigation potentially applicable to other forms of trauma and possibly even useful in determining patient risk for MIE prior to elective surgical procedures. This study provides a much-needed new direction for future clinical trials. In particular, appropriate biomarkers and additional information regarding patient health status might be essential for successful clinical trials of anti-sepsis drugs.^{21,22} Identification of the hyper-susceptible patients could enable more focused study design when expensive/invasive interventions, such as for the testing of cutting-edge technologies or products are involved by directing intervention to those who need it most. Identification of this group early after admission could also allow adjunctive treatments such as immunotherapy, extra-corporeal lipopolysaccharide removal, and other novel treatments to be tested prior to the decline of the patient's clinical status due to MIE.

We envision that the development of a comprehensive diagnostic tool set will depend on the integration of genomic signatures of both host and pathogen. The blood biomarkers reported could be further developed and integrated with other diagnostic tools, such as genomic

single nucleotide polymorphisms (SNPs) that predispose certain patients to infection,^{51,52} and produce a more comprehensive prognosis of patient susceptibility. Physician decisions rely heavily on blood tests over the course of recovery, and a positive culture is still the most accepted and reliable method for diagnosing infection. Using biomarkers, these blood samples could also allow us to monitor the changes in susceptibility status and adjust treatments accordingly. Modern molecular based microbiological tests,⁵³ such as detection of *P. aeruginosa* in wound biopsy using RT-PCR based assays,⁵⁴ have been developed but not yet widely utilized. Several molecular early detection kits have become commercially available for diagnosing common bloodstream infections, and have been found to show some promise despite of much room left for improvement.^{55,56} Our biomarkers on the host response may work synergistically with these tests to support physician decisions.

The discovery of these biomarkers and the validation of the methods pave the way for identifying biomarkers from other tissues involved in host defense, such as muscle, fat, and skin samples,⁵⁷ of which often become available from surgical procedures or wound debridement. Biomarkers from other tissues may further enhance a combined model or perhaps provide even better prognostic value than blood biomarkers and clinical characteristics.

This study is limited by the unavailability of pathogen genotyping information below species level. We could not distinguish whether a reoccurring infection was caused by persistent or MDR pathogen, and could not identify biomarkers that can potentially differentiate susceptibility to different pathogens, such as Gram positive/negative bacteria, and even to species level. Nonetheless, our 6-day window (SDC Figure 1B) was designed to minimize infection episodes caused by the same strain(s). Our definition of hyper-susceptibility is based on natural definition of having repeated infections. Changing this definition, for example, to having at least three infection episodes, did not significantly change the biomarkers identified (data not shown). However, the *P* values for differential gene expression and clinical characteristics became less significant, suggesting either the criterion is not the best cut off point to separate two different groups, or that the statistical power is reduced due to smaller number of patients in the hyper-susceptible group.

Although this work and our model focused on thermally injured trauma patients, our approach is potentially applicable to other types of trauma and surgical patients. In this study, to ensure portability of our models, we carried out rigorous internal CV to ensure robustness of our regression models. However, due to the novelty of this clinical and transcriptome dataset, independent cohort data was unavailable for CV. Although our dataset is the largest of its kind to date, the sample size is still too small to build a larger panel without risking over-fitting the model. Our genomics data warrant future trials with a larger randomized cohort study, as well as mechanistic interrogations using animal models. Our findings open new avenues for the prevention and treatment of repeated infections in critical care, and provide novel components for the development of integrated prognosis and diagnosis using biomarkers, SNPs and pathogen detection. Future studies should investigate the potential broad applicability, and assess whether early triage based on predictive models can improve outcomes of trauma patients.

Supplementary Material

Refer to Web version on PubMed Central for supplementary material.

Acknowledgements

This work was supported by the U.S. Army Medical Research Acquisition Act of U.S. Department of Defense, Congressionally Directed Medical Research Programs (CDMRP), Defense Medical Research and Development Program (DMRDP) Basic Research Award, W81XWH-10-DMRDP-BRA to LGR. The investigators acknowledge the contribution of the Inflammation and the Host Response to Injury Large-Scale Collaborative Project Award #5U54GM062119 from the National Institute of General Medical Sciences. We thank W. Xu, W. Xiao, and A. A. Tzika for suggestions on the data analysis.

Sources of support: U.S. Army Medical Research Acquisition Act of U.S. Department of Defense; National Institute of General Medical Sciences.

References

- Morris JA, MacKenzie EJ, Damiano AM, et al. Mortality in trauma patients: the interaction between host factors and severity. *J Trauma*. 1990; 30:1476–1482. [PubMed: 2258958]
- Kraft R, Herndon DN, Al-Mousawi AM, et al. Burn size and survival probability in paediatric patients in modern burn care: a prospective observational cohort study. *Lancet*. 2012; 379:1013–1021. [PubMed: 22296810]
- Ryan CM, Schoenfeld DA, Thorpe WP, et al. Objective estimates of the probability of death from burn injuries. *N Engl J Med*. 1998; 338:362–366. [PubMed: 9449729]
- Osler T, Gance L, Buzas JS, et al. A trauma mortality prediction model based on the anatomic injury scale. *Ann Surg*. 2008; 247:1041–1048. [PubMed: 18520233]
- MacKenzie EJ, Rivara FP, Jurkovich GJ, et al. A National Evaluation of the Effect of Trauma-Center Care on Mortality. *N Engl J Med*. 2006; 354:366–378. [PubMed: 16436768]
- Church D, Elsayed S, Reid O, et al. Burn wound infections. *Clin Microbiol Rev*. 2006; 19:403–434. [PubMed: 16614255]
- Bloemsma GC, Dokter J, Boxma H, et al. Mortality and causes of death in a burn centre. *Burns*. 2008; 34:1103–1107. [PubMed: 18538932]
- Ingraham AM, Xiong W, Hemmilla MR, et al. The attributable mortality and length of stay of trauma-related complications: a matched cohort study. *Ann Surg*. 2010; 252:358–362. [PubMed: 20622658]
- Kesarwani M, Hazan R, He J, et al. A quorum sensing regulated small volatile molecule reduces acute virulence and promotes chronic infection phenotypes. *PLoS Pathog*. 2011; 7:e1002192. [PubMed: 21829370]
- Bandyopadhyaya A, Kesarwani M, Que Y-A, et al. The quorum sensing volatile molecule 2-aminoacetophenone modulates host immune responses in a manner that promotes life with unwanted guests. *PLoS Pathog*. 2012; 8:e1003024. [PubMed: 23166496]
- Boucher HW, Talbot GH, Bradley JS, et al. Bad bugs, no drugs: no ESCAPE! An update from the Infectious Diseases Society of America. *Clin Infect Dis*. 2009; 48:1–12. [PubMed: 19035777]
- Avni T, Levkovich A, Ad-El DD, et al. Prophylactic antibiotics for burns patients: systematic review and meta-analysis. *BMJ (Clinical research ed.)*. 2010; 340:c241.
- Cohen NR, Lobritz MA, Collins JJ. Microbial Persistence and the Road to Drug Resistance. *Cell Host Microbe*. 2013; 13:632–642. [PubMed: 23768488]
- Pirnay J-P, De Vos D, Cochez C, et al. Molecular Epidemiology of *Pseudomonas aeruginosa* Colonization in a Burn Unit: Persistence of a Multidrug-Resistant Clone and a Silver Sulfadiazine-Resistant Clone. *J Clin Microbiol*. 2003; 41:1192–1202. [PubMed: 12624051]
- De Vos D, Lim AJ, Pirnay P, et al. Analysis of epidemic *Pseudomonas aeruginosa* isolates by isoelectric focusing of pyoverdine and RAPD-PCR: modern tools for an integrated anti-nosocomial infection strategy in burn wound centres. *Burns*. 1997; 23:379–386. [PubMed: 9426906]

16. Brunkhorst FM, Oppert M, Marx G, et al. Effect of empirical treatment with moxifloxacin and meropenem vs meropenem on sepsis-related organ dysfunction in patients with severe sepsis: a randomized trial. *JAMA*. 2012; 307:2390–2399. [PubMed: 22692171]
17. Schuetz P, Litke A, Albrich WC, et al. Blood biomarkers for personalized treatment and patient management decisions in community-acquired pneumonia. *Curr Opin Infect Dis*. 2013; 26:159–167. [PubMed: 23434895]
18. Härtel C, Deuster M, Lehrmbecher T, et al. Current approaches for risk stratification of infectious complications in pediatric oncology. *Pediatr Blood Cancer*. 2007; 49:767–773. [PubMed: 17514729]
19. Angus DC. The search for effective therapy for sepsis: back to the drawing board? *JAMA*. 2011; 306:2614–2615. [PubMed: 22187284]
20. Kuehn BM. Guideline Promotes Early, Aggressive Sepsis Treatment to Boost Survival. *JAMA*. 2013; 309:969–970. [PubMed: 23483148]
21. Schuetz P, Haubitza S, Mueller B. Do sepsis biomarkers in the emergency room allow transition from bundled sepsis care to personalized patient care? *Curr Opin Crit Care*. 2012; 18:341–349. [PubMed: 22610364]
22. Angus DC, van der Poll T. Severe sepsis and septic shock. *N Engl J Med*. 2013; 369:840–851. [PubMed: 23984731]
23. Nichols RL, Smith JW, Klein DB, et al. Risk of infection after penetrating abdominal trauma. *N Engl J Med*. 1984; 311:1065–1070. [PubMed: 6482920]
24. Kisat M, Villegas CV, Onguti S, et al. Predictors of sepsis in moderately severely injured patients: an analysis of the national trauma data bank. *Surg Infect (Larchmt)*. 2013; 14:62–68. [PubMed: 23461696]
25. Wibbenmeyer L, Danks R, Faucher L, et al. Prospective analysis of nosocomial infection rates, antibiotic use, and patterns of resistance in a burn population. *J Burn Care Res*. 2006; 27:152–160. [PubMed: 16566558]
26. Boomer JS, To K, Chang KC, et al. Immunosuppression in patients who die of sepsis and multiple organ failure. *JAMA*. 2011; 306:2594–2605. [PubMed: 22187279]
27. Lavrentieva A, Papadopoulou S, Kioumis J, et al. PCT as a diagnostic and prognostic tool in burn patients. Whether time course has a role in monitoring sepsis treatment. *Burns*. 2012; 38:356–363. [PubMed: 22037153]
28. Schultz L, Walker SAN, Elligsen M, et al. Identification of predictors of early infection in acute burn patients. *Burns*. 2013; 39:1355–1366. [PubMed: 23664774]
29. Cuenca AG, Gentile LF, Lopez MC, et al. Development of a Genomic Metric That Can Be Rapidly Used to Predict Clinical Outcome in Severely Injured Trauma Patients. *Crit Care Med*. 2013; 41:1175–1185. [PubMed: 23388514]
30. Laudanski K, Miller-Graziano C, Xiao W, et al. Cell-specific expression and pathway analyses reveal alterations in trauma-related human T cell and monocyte pathways. *Proc Natl Acad Sci U S A*. 2006; 103:15564–15569. [PubMed: 17032758]
31. Xiao W, Mindrin MN, Seok J, et al. A genomic storm in critically injured humans. *J Exp Med*. 2011; 208:2581–2590. [PubMed: 22110166]
32. Jeschke MG, Finnerty CC, Emdad F, et al. Mild Obesity Is Protective After Severe Burn Injury. *Ann Surg*. 2013 Publish Ahead of Print:1.
33. Wu Z, Irizarry RA, Gentleman R, et al. A model based background adjustment for oligonucleotide expression arrays. Johns Hopkins University, Dept. of Biostatistics Working Papers. 2004
34. Gentleman RC, Carey VJ, Bates DM, et al. Bioconductor: open software development for computational biology and bioinformatics. *Genome Biol*. 2004; 5:R80. [PubMed: 15461798]
35. Kauffmann A, Gentleman R, Huber W. arrayQualityMetrics--a bioconductor package for quality assessment of microarray data. *Bioinformatics*. 2009; 25:415–416. [PubMed: 19106121]
36. Servant N, Gravier E, Gestraud P, et al. EMA - A R package for Easy Microarray data analysis. *BMC Res Notes*. 2010; 3:277. [PubMed: 21047405]
37. Smyth GK. Linear models and empirical bayes methods for assessing differential expression in microarray experiments. *Stat Appl Genet Mol Biol*. 2004; 3 Article3.

38. Tibshirani R. Regression Shrinkage and Selection via the Lasso. *J R Stat Soc Series B Stat Methodol.* 1996; 58:267–288.
39. Friedman J, Hastie T, Tibshirani R. Regularization Paths for Generalized Linear Models via Coordinate Descent. *J Stat Softw.* 2010; 33:1–22. [PubMed: 20808728]
40. Huang DW, Sherman BT, Stephens R, et al. DAVID gene ID conversion tool. *Bioinformatics.* 2008; 24:428–430. [PubMed: 18841237]
41. Wacharasint P, Boyd JH, Russell JA, et al. One size does not fit all in severe infection: obesity alters outcome, susceptibility, treatment, and inflammatory response. *Crit Care.* 2013; 17:R122. [PubMed: 23786836]
42. Johnson CA, Kleshchenko YY, Ikejiani AO, et al. Thrombospondin-1 Interacts with Trypanosoma cruzi Surface Calreticulin to Enhance Cellular Infection. *PLoS One.* 2012; 7:e40614. [PubMed: 22808206]
43. McMaken S, Exline MC, Mehta P, et al. Thrombospondin-1 Contributes to Mortality in Murine Sepsis through Effects on Innate Immunity. *PLoS One.* 2011; 6:e19654. [PubMed: 21573017]
44. Streit M, Velasco P, Riccardi L, et al. Thrombospondin-1 suppresses wound healing and granulation tissue formation in the skin of transgenic mice. *EMBO J.* 2000; 19:3272–3282. [PubMed: 10880440]
45. Shannon O. Platelets interact with bacterial pathogens. *Thromb Haemost.* 2009; 102:613–614. [PubMed: 19806244]
46. Carson WF, Cavassani KA, Dou Y, et al. Epigenetic regulation of immune cell functions during post-septic immunosuppression. *Epigenetics.* 2011; 6:273–283. [PubMed: 21048427]
47. Smale ST. Selective transcription in response to an inflammatory stimulus. *Cell.* 2010; 140:833–844. [PubMed: 20303874]
48. Perez-Campo FM, Costa G, Lie-a-Ling M, et al. The MYSTERIOUS MOZ, a histone acetyltransferase with a key role in haematopoiesis. *Immunology.* 2013; 139:161–165. [PubMed: 23347099]
49. De Santa F, Narang V, Yap ZH, et al. Jmjd3 contributes to the control of gene expression in LPS-activated macrophages. *EMBO J.* 2009; 28:3341–3352. [PubMed: 19779457]
50. Kruidenier L, Chung C-W, Cheng Z, et al. A selective jumonji H3K27 demethylase inhibitor modulates the proinflammatory macrophage response. *Nature.* 2012; 488:404–408. [PubMed: 22842901]
51. Netea MG, Wijmenga C, O'Neill LAJ. Genetic variation in Toll-like receptors and disease susceptibility. *Nat Immunol.* 2012; 13:535–542. [PubMed: 22610250]
52. Bronkhorst MWGA, Lomax MAZ, Vossen RHAM, et al. Risk of infection and sepsis in severely injured patients related to single nucleotide polymorphisms in the lectin pathway. *Br J Surg.* 2013; 100:1818–1826. [PubMed: 24227370]
53. Jannes G, De Vos D. A review of current and future molecular diagnostic tests for use in the microbiology laboratory. *Methods Mol Biol.* 2006; 345:1–21. [PubMed: 16957343]
54. Pirnay J-P, De Vos D, Duinslaeger L, et al. Quantitation of Pseudomonas aeruginosa in wound biopsy samples: from bacterial culture to rapid 'real-time' polymerase chain reaction. *Crit Care.* 2000; 4:255. [PubMed: 11056755]
55. Chang S-S, Hsieh W-H, Liu T-S, et al. Multiplex PCR system for rapid detection of pathogens in patients with presumed sepsis - a systemic review and meta-analysis. *PLoS One.* 2013; 8:e62323. [PubMed: 23734173]
56. Skvarc M, Stubljar D, Rogina P, et al. Non-culture-based methods to diagnose bloodstream infection: Does it work? *Eur J Microbiol Immunol (Bp).* 2013; 3:97–104. [PubMed: 24265925]
57. Apidianakis Y, Que YA, Xu W, et al. Down-regulation of glutathione S-transferase 4 (hGSTA4) in the muscle of thermally injured patients is indicative of susceptibility to bacterial infection. *FASEB J.* 2012; 26:730–737. [PubMed: 22038048]

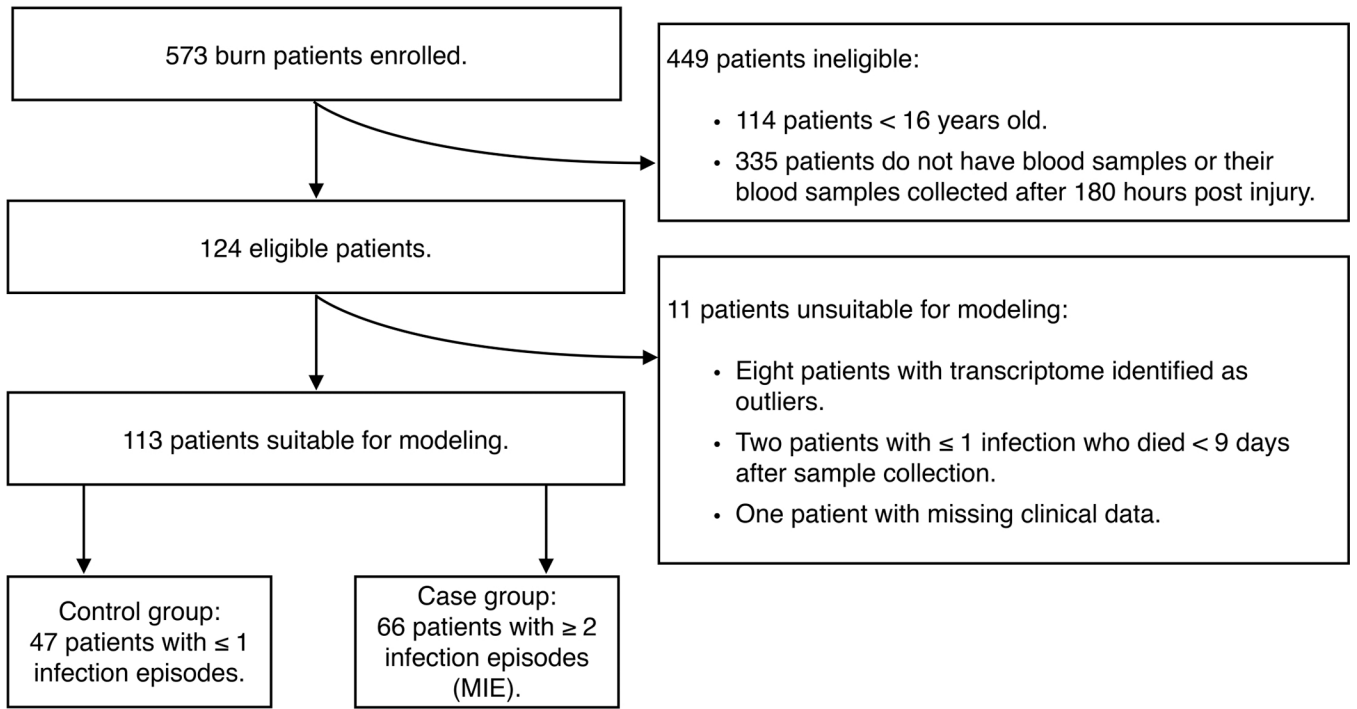


Figure 1. Sample selection process

^aDevelopment of predictive models and discovery of biomarkers.

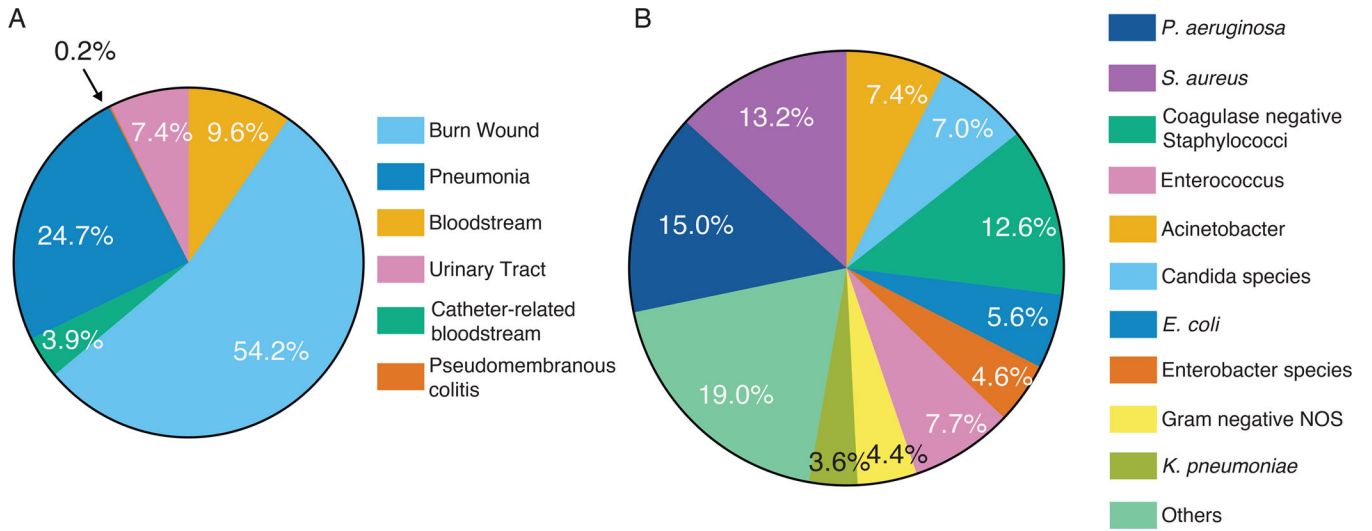


Figure 2. Type of infections and isolated pathogens
A. Types of infection. One case of pseudomembranous colitis represents 0.2%. **B.** The percentage of isolated pathogens among all infection records.

Author Manuscript

Author Manuscript

Author Manuscript

Author Manuscript

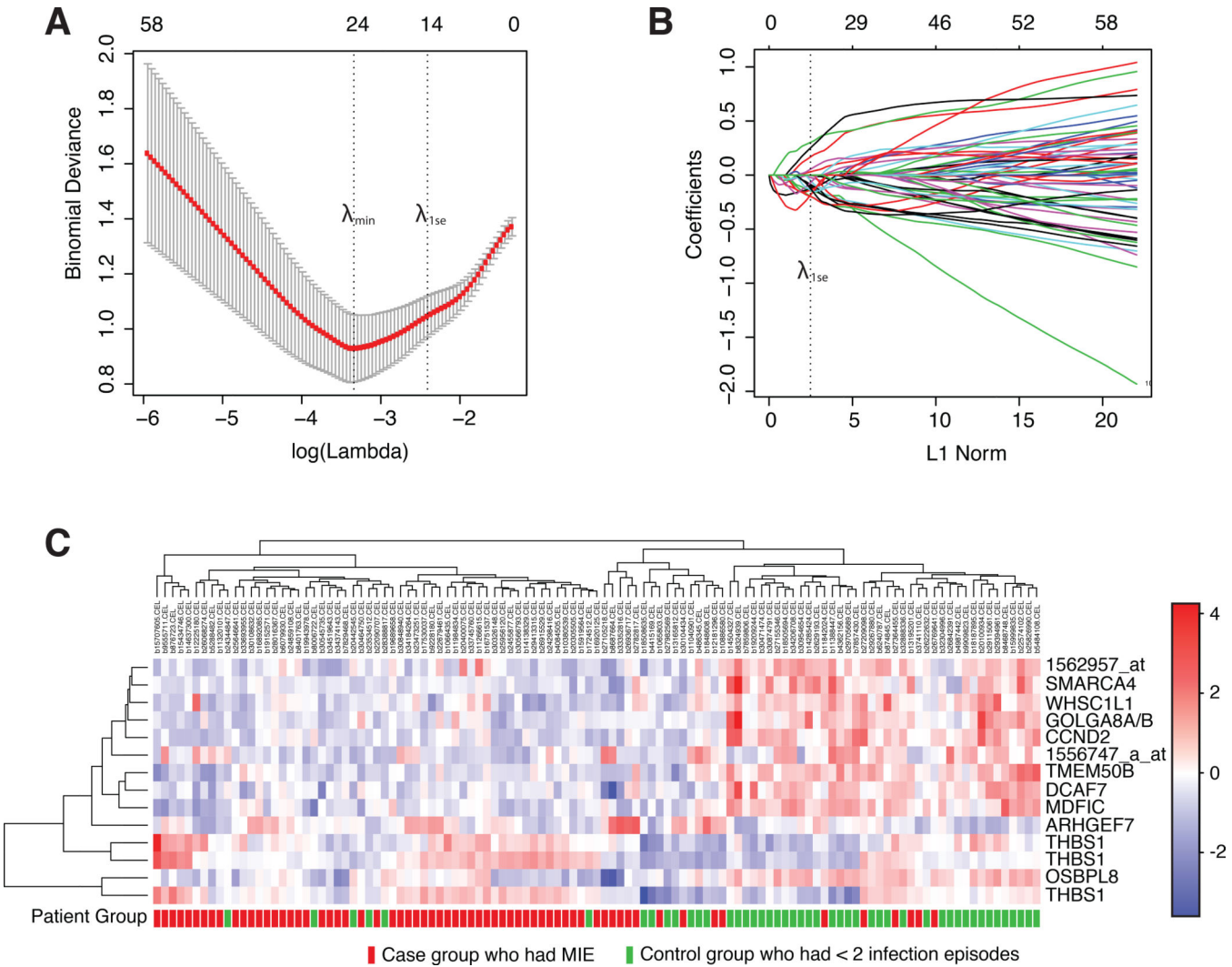


Figure 3. Clinical and genomic prediction models
 ROC curves of the clinical model, genomic model, and combined model, and their respective AUROC, cross-validated (CV) AUROC, sensitivities, and specificities; 95% CIs are reported in parentheses. The blue, orange, and black lines are the ROC curves for the biomarker panel model, clinical model, and combined model, respectively.

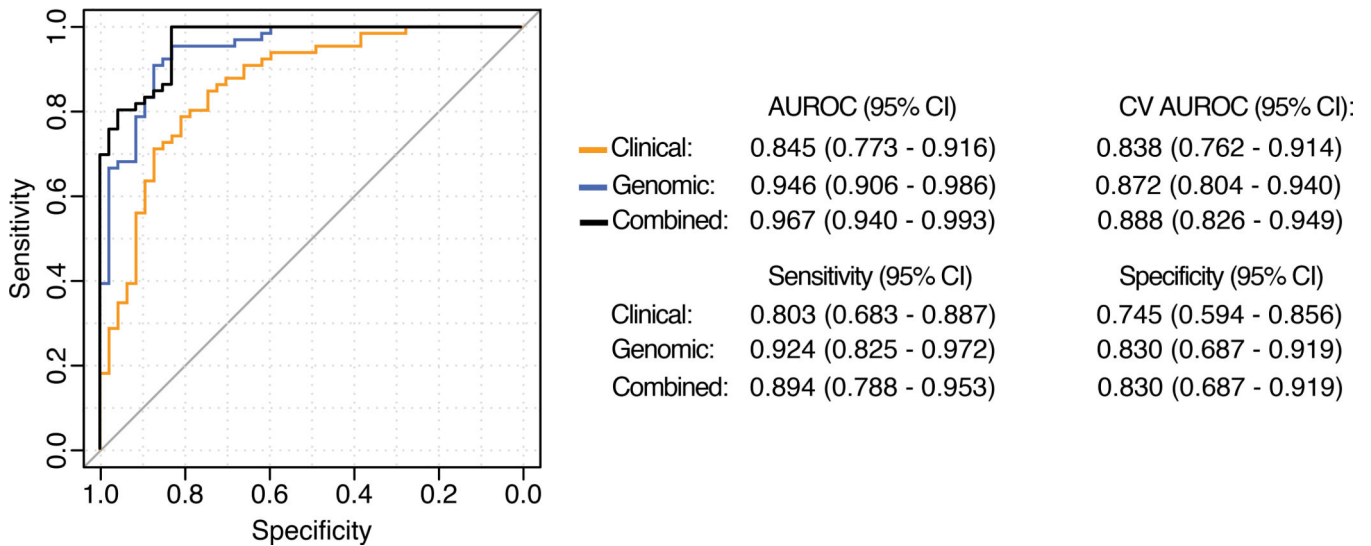


Figure 4. Biomarker selection by LASSO regularized regression

A. A representative repetition of 10-fold CV LASSO that chose 14 probe sets at λ_{1se} . The first vertical dotted line corresponds to the λ_{min} that minimized binomial deviance during CV. The second dotted line corresponds to λ_{1se} , used for the selection of 14 probe sets as shown in **B.** **B.** LASSO coefficient profile plot of the coefficient paths. At λ_{1se} , as shown with the dotted line, 14 probe sets have their coefficients significantly different from zero and thus were chosen as part of the biomarker panel. **C.** Heat map showing the expression levels of the 14 probe sets selected by LASSO as covariates for the genomic model. Each column corresponds to one of the 113 patient samples. Each row corresponds to one of the 14 probe sets. Whenever available, gene names were provided (see Table 2 for Affymetrix probe identification). The heat map color-coding is based on probe-set-specific, re-normalized expression values, with red signifying upregulation, blue signifying down-regulation, and white indicating no difference in the hyper-susceptible patients compared to the controls. Patients that developed MIE are labeled red and those that had <2 infection episodes are labeled green at the bottom of the heat map.

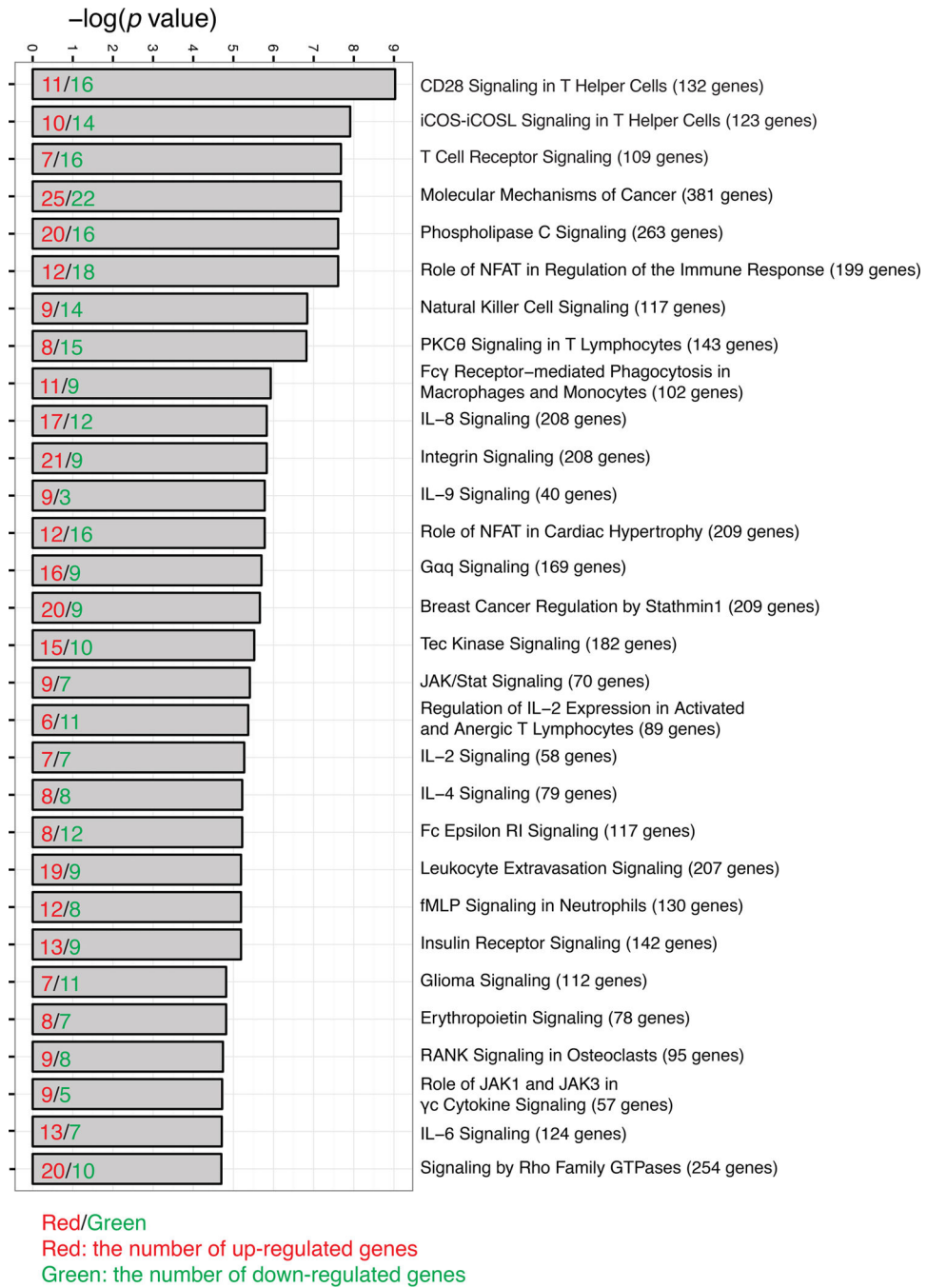


Figure 5. Pathways significantly altered

Top 30 pathways significantly altered in case group with MIE. X-axis is the negative log *P* value calculated from Fisher's exact test right-tailed. Red/Green inside bars are the number of upregulated/down-regulated genes. The total number of genes in a pathway is indicated in the parenthesis after pathway name. *P* value is calculated by Fisher's exact test by IPA software.

Table 1

Demographics and clinical characteristics of participants.

| | All (n=113) | Controls (1 Infectious Episodes) (n=47) | Cases (2 Infectious Episodes [MIE]) (n=66) | P value |
|-------------------------------------------------------|-------------|---------------------------------------------------|---------------------------------------------------------|---------|
| Age when injured, mean (SD), y | 37.7 (15.6) | 37.0 (14.6) | 38.2 (16.4) | 0.681 |
| Sex, n (%) males | 90 (79.6%) | 40 (85.1%) | 50 (75.8%) | 0.218 |
| BMI Category, n (%) | | | | 0.888 |
| Underweight | 5 (4.4%) | 1 (2.1%) | 4 (6.1%) | |
| Healthy | 44 (38.9%) | 19 (40.4%) | 25 (37.9%) | |
| Overweight | 35 (31.0%) | 15 (31.9%) | 20 (30.3%) | |
| Obese | 29 (25.7%) | 12 (25.6%) | 17 (25.8%) | |
| Severity of Injury | | | | |
| APACHE II Score, median (IQR) | 20 (12–26) | 13 (8–20) | 24 (18–28) | <0.001* |
| Burns size of TBSA, % (IQR) | 40 (28–56) | 32 (23–40) | 46 (35–70) | <0.001* |
| Presence of Inhalation Injury, n (%) | 49 (43.4%) | 8 (17.0%) | 41 (62.1%) | <0.001* |
| Outcome | | | | |
| Hospital Stay, d (IQR) | 35 (19–62) | 20 (15–27) | 60 (33–71) | <0.001* |
| Hospital Stay of Survived, d (IQR) | 36 (19–62) | 20.5 (15–27) | 61 (44–72) | <0.001* |
| Days on Ventilation, d (IQR) | 13 (2–33) | 2 (0–5) | 28 (13–40) | <0.001* |
| Day of Death Since Injury, d (IQR) | 34 (18–63) | 21 (18–21) | 35.5 (18–65) | 0.3753 |
| Mortality, no. (%) | 21 (18.6%) | 3 (6.38%) | 18 (27.3%) | 0.0029* |
| Number of Records by Type of Infection, n (%) | | | | |
| Burn wound | 332 (54.2%) | 24 (60%) | 308 (53.8%) | |
| Pneumonia | 151 (24.7%) | 8 (20%) | 143 (25.0%) | |
| Bloodstream | 59 (9.6%) | 1 (2.5%) | 58 (10.1%) | |
| Urinary tract | 45 (7.4%) | 7 (17.5%) | 38 (6.6%) | |
| Catheter-related bloodstream | 24 (3.9%) | 0 (0%) | 24 (4.2%) | |
| Pseudomembranous colitis | 1 (0.2%) | 0 (0%) | 1 (0.2%) | |
| Number of Records by Isolated Pathogens, n (%) | | | | |
| <i>P. aeruginosa</i> | 92 (15.0%) | 4 (10%) | 88 (15.4%) | |
| <i>S. aureus</i> | 81 (13.2%) | 7 (17.5%) | 74 (13.0%) | |
| Coagulase negative Staphylococci | 77 (12.6%) | 6 (15.0%) | 71 (12.4%) | |
| Enterococcus | 47 (7.7%) | 4 (10.0%) | 43 (7.5%) | |
| Acinetobacter | 45 (7.4%) | 1 (2.5%) | 44 (7.7%) | |
| Candida species | 43 (7.0%) | 0 (0%) | 43 (7.5%) | |
| <i>E. coli</i> | 34 (5.6%) | 1 (2.5%) | 33 (5.8%) | |
| Enterobacter species | 28 (4.6%) | 1 (2.5%) | 27 (4.7%) | |

| | All (n=113) | Controls (1 Infectious Episodes) (n=47) | Cases (2 Infectious Episodes [MIE]) (n=66) | P value |
|-----------------------------|-------------|---------------------------------------------------|---------------------------------------------------------|---------|
| Gram negative NOS | 27 (4.4%) | 0 (0%) | 27 (4.7%) | |
| <i>K. pneumoniae</i> | 22 (3.6%) | 0 (0%) | 22 (3.8%) | |
| Others | 116 (18.9%) | 16 (40%) | 100 (17.5%) | |

* $P < 0.05$.

Abbreviations: BMI, body mass index; IQR, inter-quartile range; TBSA, total body surface area.

Author Manuscript

Author Manuscript

Author Manuscript

Author Manuscript

Table 2

The 14 probe sets in the biomarker panel.

| Probe set | Gene Symbol | Gene Name | Gene Ontology Biological Process Annotation | Fold Change | Coefficients | P value |
|-----------------------|-----------------|---------------------------------------------------------------------------------------------------|------------------------------------------------------------------------------------------------------------------------------------------------------------------------------------------------------------------------|-------------|--------------|---------|
| Upregulated | | | | | | |
| 201109_s_at | THBS1 | thrombospondin 1 | Angiogenesis, regulation of cytokine production, regulation of endothelial cell proliferation, regulation of antigen processing and presentation, regulation of immune system process | 3.37 | 0.560 | <0.001 |
| 201110_s_at | THBS1 | thrombospondin 1 | Same as above | 2.31 | 0.100 | 0.001 |
| 201108_s_at | THBS1 | thrombospondin 1 | Same as above | 2.02 | 0.824 | 0.001 |
| 235412_at | ARHGEF7 | Rho guanine nucleotide exchange factor (GEF) 7 | Apoptotic process, signal transduction, epidermal growth factor receptor signaling pathway, small GTPase mediated signal transduction, apoptotic signaling pathway, lamellipodium assembly | 1.86 | 0.747 | 0.017 |
| Down-regulated | | | | | | |
| 217599_s_at | MDFC | MyoD family inhibitor domain containing | Transcription, activation of JUN kinase activity, virus-host interaction, regulation of Wnt receptor signaling pathway, negative regulation of protein import into nucleus, positive regulation of viral transcription | -2.34 | -0.289 | <0.001 |
| 200951_s_at | CCND2 | cyclin D2 | Positive regulation of cyclin-dependent protein kinase activity, cell cycle, cell division | -2.21 | 0.292 | <0.001 |
| 228986_at | OSBPL8 | oxysterol binding protein-like 8 | Lipid transport, negative regulation of sequestering of triglyceride, fat cell differentiation | -1.98 | 0.111 | <0.001 |
| 224730_at | DCAF7 | DDB1 and CUL4 associated factor 7 | Multicellular organismal development, protein ubiquitination | -1.87 | -0.908 | <0.001 |
| 222907_x_at | TMEM50B | transmembrane protein 50B | NA | -1.80 | -0.335 | <0.001 |
| 208797_s_at | GOLGA8A/GOLGA8B | golgin A8 family, member B | NA | -1.78 | -1.068 | <0.001 |
| 217656_at | SMARCA4 | SWI/SNF related, matrix associated, actin dependent regulator of chromatin, subfamily a, member 4 | Negative regulation of transcription from RNA polymerase II promoter, chromatin remodeling, negative regulation of cell growth, negative regulation of androgen receptor signaling pathway, etc. | -1.59 | 0.252 | <0.001 |
| 221248_s_at | WHSC1L1 | Wolf-Hirschhorn syndrome candidate 1-like 1 | Transcription, regulation of transcription, cell growth, histone methylation, cell differentiation, histone lysine methylation | -1.51 | -0.676 | <0.001 |
| 1556747_a_at | NA | NA | NA | -1.66 | -0.786 | 0.005 |
| 1562957_at | NA | NA | NA | -1.64 | -0.409 | <0.001 |

P values were adjusted for multiple comparisons based on Benjamini-Hochberg method during the fold-change calculation of 26,107 probes after initial filtering (see Methods).

Table 3

Predicted early functional changes in case group that had MIE.

| Functions annotation | <i>P</i> value | Activation z-score | # of genes |
|--------------------------------------|----------------|--------------------|------------|
| Increased | | | |
| Chemotaxis | <0.001 | 3.924 | 55 |
| Chemotaxis of cells | <0.001 | 3.924 | 54 |
| Homing of cells | <0.001 | 3.815 | 59 |
| Chemotaxis of leukocytes | <0.001 | 3.795 | 37 |
| Chemotaxis of phagocytes | <0.001 | 3.546 | 30 |
| Chemotaxis of myeloid cells | <0.001 | 3.501 | 29 |
| Homing of leukocytes | <0.001 | 3.484 | 41 |
| Replication of Influenza A virus | <0.001 | 3.413 | 38 |
| Replication of virus | <0.001 | 3.314 | 64 |
| Leukocyte migration | <0.001 | 3.088 | 100 |
| Inflammatory response | <0.001 | 3.085 | 72 |
| Viral infection | <0.001 | 3.046 | 166 |
| Cytostasis | <0.001 | 2.913 | 30 |
| Replication of RNA virus | <0.001 | 2.782 | 56 |
| Cell movement | <0.001 | 2.766 | 173 |
| Migration of cells | <0.001 | 2.619 | 161 |
| Tyrosine phosphorylation of protein | <0.001 | 2.456 | 29 |
| Recruitment of cells | <0.001 | 2.451 | 34 |
| Recruitment of granulocytes | <0.001 | 2.405 | 26 |
| Polarization of leukocytes | <0.001 | 2.337 | 13 |
| Recruitment of leukocytes | <0.001 | 2.333 | 33 |
| Adhesion of immune cells | <0.001 | 2.271 | 40 |
| Recruitment of myeloid cells | <0.001 | 2.263 | 27 |
| Adhesion of blood cells | <0.001 | 2.250 | 41 |
| Cell viability | <0.001 | 2.240 | 112 |
| Orientation of macrophages | <0.001 | 2.200 | 6 |
| Attachment of cells | <0.001 | 2.166 | 18 |
| Disassembly of focal adhesions | <0.001 | 2.164 | 7 |
| Formation of membrane ruffles | <0.001 | 2.137 | 12 |
| Cell survival | <0.001 | 2.101 | 121 |
| Cell movement of neutrophils | <0.001 | 2.067 | 37 |
| Invasion of breast cancer cell lines | <0.001 | 2.064 | 25 |
| Orientation of cells | <0.001 | 2.028 | 19 |
| Decreased | | | |
| Development of lymphoid organ | <0.001 | -3.241 | 30 |

| Functions annotation | P value | Activation z-score | # of genes |
|-------------------------------------------|----------------|---------------------------|-------------------|
| Development of lymphatic system component | <0.001 | -2.970 | 41 |
| Bacterial infection | <0.001 | -2.890 | 47 |
| Expansion of leukocytes | <0.001 | -2.753 | 25 |
| Expansion of lymphocytes | <0.001 | -2.635 | 21 |
| Development of lymph node | <0.001 | -2.608 | 14 |
| Morphology of germinal center | <0.001 | -2.415 | 11 |
| Morphology of lymph follicle | <0.001 | -2.415 | 15 |
| Expansion of blood cells | <0.001 | -2.384 | 26 |
| Encephalitis | <0.001 | -2.374 | 27 |
| Inflammation of organ | <0.001 | -2.362 | 97 |
| Quantity of neutrophils | 0.0011 | -2.208 | 23 |
| Development of thymocytes | <0.001 | -2.189 | 13 |
| Quantity of granulocytes | <0.001 | -2.133 | 36 |
| Organismal death | <0.001 | -2.074 | 196 |

An absolute z-score of 2 was designated as significant by the IPA software. The numbers of genes used to predict functional changes are indicated in the column with the heading “# of genes”.